

## Vibrational Analysis of *trans*-1,4-Polypentadiene. 2. Deuterio Derivatives and Interchain Interaction

N. Neto\*

*Centro di Studio Sulla Chimica e Struttura dei Composti Eterociclici, CNR, 50121 Firenze, Italy*

M. Muniz-Miranda

*Istituto di Chimica Fisica, Università di Firenze, 50121 Firenze, Italy*

E. Benedetti

*Centro di Studio per le Macromolecole Stereordinate ed Otticamente Attive, CNR, 56100 Pisa, Italy. Received January 15, 1980*

**ABSTRACT:** The infrared spectra of the  $d_2$  and  $d_8$  derivatives of isotactic *trans*-1,4-poly(1,3-pentadiene) are reported, and the absorption frequencies are compared with values calculated using a set of force constants for the intrachain potential and semiempirical atom-atom functions to account for interaction among chains. Calculations are carried out by a formalism which does not include first derivatives of atom-atom potential since, as pointed out in the theoretical section, this inclusion may produce an inconsistency in the treatment. Previous results based on an isolated-chain model are confirmed and the vibrational assignment is extended to the spectra of the deuterio derivatives. Calculations are presented for two different crystal structures in which the methyl groups are in a *cis* or skew conformation with respect to adjacent double bonds, but satisfactory agreement between calculated and observed spectra is obtained only for the skew conformation.

In the preceding paper,<sup>1</sup> the infrared spectra of isotactic *trans*-1,4-poly(1,3-pentadiene) (ITPP) was analyzed by using results of a normal-mode calculation for the isolated polymer chain, based on a set of force constants transferred from polybutadiene.<sup>2</sup> As pointed out in ref 1, the addition of interchain interactions should not greatly modify the conclusions of the single-chain model. In fact the spectrum of the crystalline sample is very similar to that of the paracrystalline modification in which three-dimensional order is lost and, although the crystal structure predicts four repeat units per unit cell, only a few bands show detectable factor group splitting in the low-temperature spectrum.

It is evident, however, that a quantitative check of the effects due to interchain interaction is necessary before an unambiguous assignment of the observed spectrum can be given. This is particularly true for ITTP for which two different chain conformations of small energy difference, *cis* and skew according to the description given in ref 1, are possible. Any conclusion about the more probable chain geometry may in fact be criticized in view of the exclusion of interchain potential which may favor a packing of macromolecules in a given conformation. On the other hand, since only a few frequencies show marked differences in the numerical values calculated for the two different conformations, the better overall agreement obtained in ref 1 between observed and calculated spectra for the skew form needs further spectroscopic evidence before it may be considered a reasonable suggestion for the chain geometry in the crystal.

For these reasons we undertake in the present paper a vibrational analysis of crystalline ITTP, add atom-atom interchain potential to the intrachain force constants used in ref 1, and extend the study to two deuterio derivatives, namely, isotactic *trans*-1,4-poly(1,3-pentadiene-1,1- $d_2$ ) (ITTP- $d_2$ ) and *trans*-1,4-poly(1,3-pentadiene-1,1,2,3,4,5,5,5- $d_8$ ) (ITTP- $d_8$ ). Infrared data on the deuterio derivatives are reported and compared with corresponding values calculated<sup>1</sup> with the single-chain model in order to conform to the description of normal modes previously given for ITTP. The general theory is extended to include

interchain potential and calculated frequencies, classified according to the irreducible representation of the space group of ITTP for  $\mathbf{k} = 0$ , are given for crystalline polypentadiene and its deuterio derivatives.

### Experimental Section

ITTP- $d_2$  was obtained by stereospecific polymerization of the *trans* monomer  $D_2C=CHCH=CHCH_3$ , following a procedure described in ref 3, while ITTP- $d_8$  was prepared by the method given in ref 4, starting from the fully deuterated *trans* isomer of pentadiene. Samples were handled as indicated in ref 1; the infrared spectra in the absorption region above  $600\text{ cm}^{-1}$  for both the crystalline and melted samples are reported in Figures 1 and 2 for ITTP- $d_2$  and ITTP- $d_8$ , respectively. The infrared spectrum of the crystalline sample of ITTP- $d_8$  at liquid nitrogen temperature is also given in Figure 2; it was not possible to record the corresponding spectrum of the  $d_2$  derivative due to the limited amount of sample available. As the absorption pattern in the low-frequency region is the most significant for establishing the conformation of the polymer chain, we give in Figure 3 a comparison of the spectra of all three isotopic species of ITTP in this region.

### Interchain Interaction

The theory presented in the previous paper for normal-mode calculations of an isolated polymer chain will be now extended to include interactions among chains in terms of an atom-atom potential of the kind

$$V_1 = \sum_k f_k(r_k) \quad (1)$$

$r_k$  is the distance between two atoms of two different repeat units belonging, in turn, to two different polymer chains since interactions within each chain are accounted for as described in ref 1. The sum in eq 1 extends over all possible different atom-atom distances and a subscript in  $f_k$  is used since, in general, a parametric semiempirical functional form is assumed in which parameters are specific to the atomic couple involved. If  $V$  is the intrachain potential considered in ref 1 in terms of force constants of each polymer chain, the total potential function  $V_T$  for

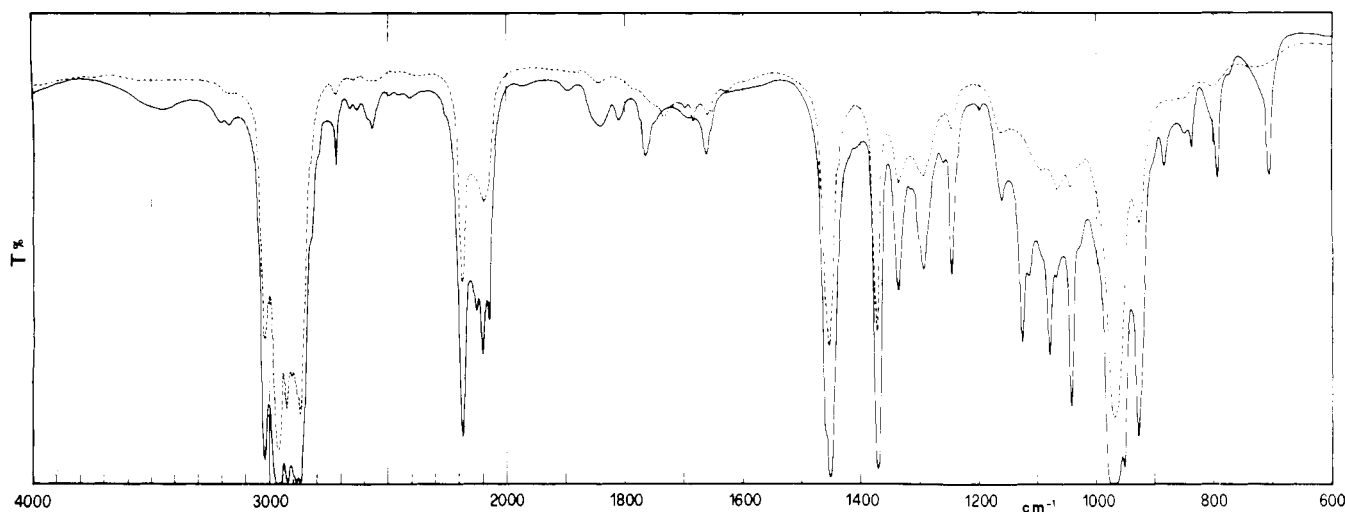


**Figure 1.** Infrared spectra of isotactic *trans*-1,4-poly(1,3-pentadiene-1,1-*d*<sub>2</sub>): (—) crystalline sample at room temperature; (---) melted sample.

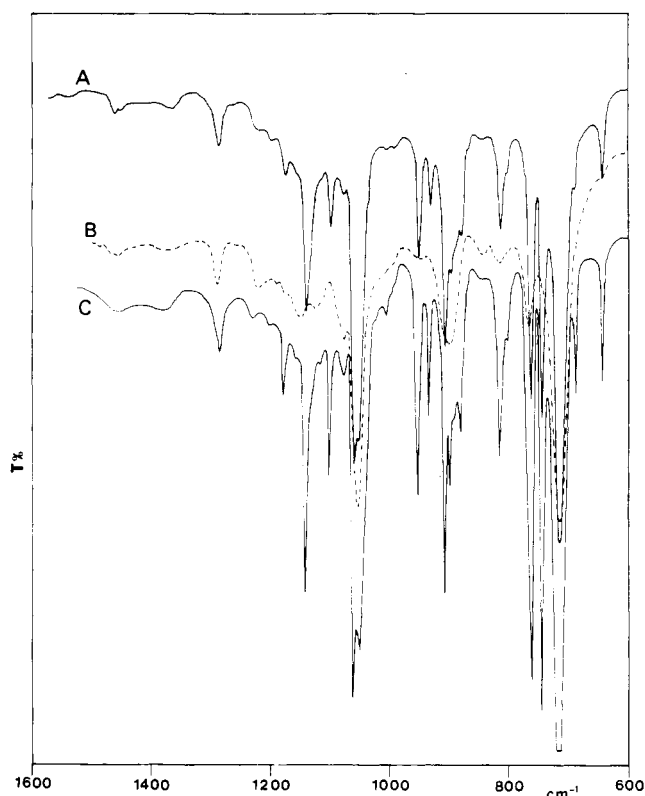


**Figure 2.** Infrared spectra of fully deuterated isotactic *trans*-1,4-polypentadiene: (A) crystalline sample at room temperature; (B) melted sample; (C) crystalline sample at liquid nitrogen temperature.

the crystalline polymer is taken here as

$$V_T = V + V_I \quad (2)$$

Under the assumption that  $V_T$  has a minimum when the crystal is at the initial (equilibrium) configuration, we have

$$(\partial V_T / \partial q_a^{\mu m})_0 = 0 \quad \text{for all } a, \mu, m \quad (3)$$

where  $q_a^{\mu m}$  is an independent displacement coordinate for the repeat unit  $\mu$  in the unit cell  $m$ , defined as in ref 1 with the obvious addition of a second superscript to account for the presence of different chains in the crystal. Since the metric tensor for rectilinear displacement coordinates  $q_a^{\mu m}$  is completely defined in ref 1, the equilibrium conditions

(3) may also be written in the alternative form

$$\left( \frac{\partial V_T}{\partial U_{is}^{\mu m}} \right) = \left( \frac{\partial V}{\partial U_{is}^{\mu m}} \right)_0 + \left( \frac{\partial V_I}{\partial U_{is}^{\mu m}} \right)_0 = 0 \quad (4)$$

in terms of mass-weighted displacements  $U_{is}^{\mu m} = m_i^{1/2} \Delta X_{is}^{\mu m}$ .

Due to the fact that an explicit functional form is not known for the intrachain potential  $V$ , the equilibrium conditions (4) amount to a formal definition of the first derivatives of  $V$  as

$$\left( \frac{\partial V}{\partial U_{is}^{\mu m}} \right)_0 \equiv \sum_p \left( \frac{\partial V}{\partial S_p} \right)_0 \left( \frac{\partial S_p}{\partial U_{is}^{\mu m}} \right)_0 = - \sum_k f_k' \left( \frac{\partial r_k}{\partial U_{is}^{\mu m}} \right)_0 \quad (5)$$

where  $S_p$  is an internal coordinate within a polymer chain in terms of which basic force constants are given according to ref 1 and  $f_k' = (\partial f_k / \partial r_k)_0$ .

Force constants for independent displacements of each repeat unit are

$$\left( \frac{\partial^2 V_T}{\partial q_a^{\mu m} \partial q_b^{\nu n}} \right)_0 = \sum_{is} \sum_{jt} \left( \frac{\partial U_{is}^{\mu m}}{\partial q_a^{\mu m}} \right)_0 \left( \frac{\partial U_{jt}^{\nu n}}{\partial q_b^{\nu n}} \right)_0 \left( \frac{\partial^2 V_T}{\partial U_{is}^{\mu m} \partial U_{jt}^{\nu n}} \right)_0 \quad (6)$$

where tensor transformation coefficients are defined as in ref 1 and Cartesian force constants are, under the assumption of eq 2 and using linear displacement coordinates

$$\left( \frac{\partial^2 V_T}{\partial U_{is}^{\mu m} \partial U_{jt}^{\nu n}} \right)_0 = \sum_{pq} \left( \frac{\partial S_p}{\partial U_{is}^{\mu m}} \right)_0 \left( \frac{\partial S_q}{\partial U_{jt}^{\nu n}} \right)_0 \left( \frac{\partial^2 V}{\partial S_p \partial S_q} \right)_0 + \sum_k \left( \frac{\partial r_k}{\partial U_{is}^{\mu m}} \right)_0 \left( \frac{\partial r_k}{\partial U_{jt}^{\nu n}} \right)_0 f_k'' \quad (7)$$

Obviously force constants appearing in the first term of the right-hand side of the eq 7 are defined only within a

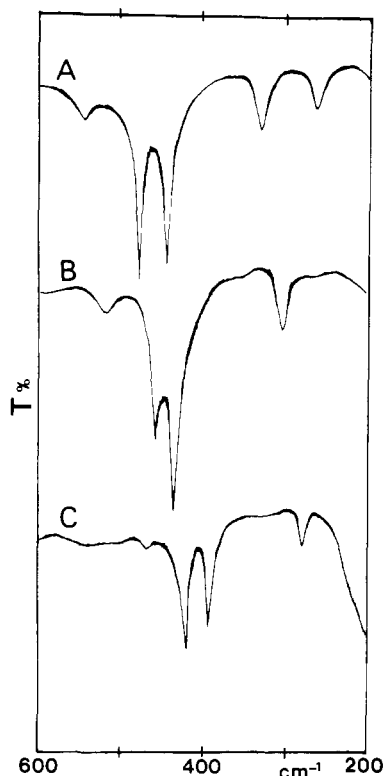


Figure 3. Low-frequency region, room-temperature infrared spectra of isotactic *trans*-1,4-polypentadiene (A) and its  $d_2$  (B) and  $d_8$  (C) deuterio derivatives.

given chain and do not contribute to Cartesian force constants for which  $\mu \neq \nu$ .

It must be pointed out that only second derivatives  $f_k'' = (\partial^2 f_k / \partial^2 r_k)_0$  appear in eq 7, while in other normal-mode calculations of polymers (see, for instance, ref 5) first derivatives  $f_k'$  are also included. The presence of  $f_k'$  is due to the expansion of each atom-atom distance  $r_k$  to second order in Cartesian displacements, such that an extra term of the kind

$$\sum_k f_k' \left( \frac{\partial^2 r_k}{\partial U_{is}^{\mu m} \partial U_{jt}^{\nu n}} \right)_0 \quad (8)$$

is added to eq 7. In this way the resulting force constants are, as explicitly stated by Kobayashi,<sup>5</sup> those obtained by assuming a simple quadratic form for  $V$  in terms of coordinates  $S_p$  and equilibrium conditions reduce to

$$\left( \frac{\partial V_I}{\partial U_{is}^{\mu m}} \right)_0 = 0 = \sum_k f_k' \left( \frac{\partial r_k}{\partial U_{is}^{\mu m}} \right)_0 \quad (9)$$

rather than the more general conditions (5). We note, however, that, when an explicit atom-atom potential function is used for  $V_I$ , eq 9 may not be, and usually is not, obeyed and this causes an inconsistency when the term (8) is included in the dynamical equation.

For instance, it is not difficult to prove, using arguments given in ref 6, that Born-Huang conditions for rotational invariance of  $V_T$  are satisfied using Cartesian force constants as given by eq 7. This is no more true when one adds a term given by (8) to (7) if conditions (9) are not strictly obeyed.

Thus the inclusion of a term of the kind (8) may produce a potential energy matrix which is not invariant under an infinitesimal rotation of the whole crystal, and this result has a counterpart if we regard each displacement  $\Delta r_k$  as an internal, dependent coordinate expanded in terms of

Table I  
Observed Spectrum and Values Calculated ( $\text{cm}^{-1}$ ) for Both Cis and Skew Forms of an Isolated Chain of Polypentadiene- $d_2$  and Assignment on the Basis of Potential Energy Distribution

obsd	calcd		potl energy distrib
	cis form	skew form	
	3027	3027	$l$ (97)
3012	3009	3009	$l$ (100)
	2961	2961	$r$ (99)
2960	2961	2961	$r$ (99)
2920	2904	2905	$s$ (98)
2870	2882	2882	$r$ (99)
2180	2184	2184	$d$ (98)
2090	2082	2082	$d$ (98)
1660	1653	1656	$D$ (67), $\varphi\psi$ (14), $T$ (14)
1455	1460	1459	$\alpha\beta$ (97)
1450	1459	1459	$\alpha\beta$ (99)
1370	1379	1379	$\alpha\beta$ (93)
1335	1339	1329	$\eta\chi$ (68)
	1316	1310	$\eta\chi$ (54), $\varphi\psi$ (13), $\tau_T$ (12)
1293	1276	1293	$\varphi\psi$ (52), $\epsilon\varphi\psi$ (14), $D$ (15)
1244	1217	1217	$\varphi\psi$ (31), $T$ (24), $\alpha\beta$ (15), $\pi$ (12)
1160	1168	1164	$\varphi\psi$ (25), $T$ (22), $\eta\chi$ (22), $\alpha\beta$ (12)
1126	1144	1141	$\epsilon\varphi\psi$ (20), $\alpha\beta$ (16), $T$ (14), $\eta\chi$ (10), $\vartheta$ (10)
1110	1103	1108	$T$ (49), $\vartheta$ (17), $\varphi\psi$ (11), $\alpha\beta$ (10)
1079	1053	1089	$z$ (44), $\pi$ (10)
1041	1043	1045	$\delta$ (87)
970	982	983	$\tau_D$ (41), $\Gamma$ (40), $\tau_T$ (17)
950	970	965	$T$ (26), $\vartheta$ (22), $\alpha\beta$ (21), $\eta\chi$ (11)
928	940	938	$\alpha\beta$ (38), $T$ (23), $\eta\chi$ (12)
883	864	874	$\vartheta$ (32), $\Gamma$ (21), $\alpha\beta$ (15)
836	854	836	$\vartheta$ (39), $\Gamma$ (35)
792	772	790	$\Gamma$ (67), $z$ (16)
705	696	703	$\Gamma$ (47), $\tau_T$ (21), $\vartheta$ (15)
515	596	527	$\epsilon\varphi\psi$ (31), $\text{rot}$ (23), $\vartheta$ (14)
452	435	434	$\epsilon\varphi\psi$ (31), $\pi$ (19), $\eta\chi$ (14), $\text{rot}$ (10), $\tau_T$ (10)
433	393	430	$\pi$ (50), $\Gamma$ (24), $\tau_T$ (11)
300	292	308	$\text{rot}$ (49), $\tau_T$ (36)
198	218	204	$\tau_z$ (30), $\tau_T$ (30), $\text{rot}$ (12)
	191	189	$\tau_z$ (39), $\epsilon\varphi\psi$ (17), $\text{rot}$ (16)
	170	176	$\tau_T$ (81), $\text{rot}$ (14)

the independent set  $q_a^{\mu m}$ . Since the  $q_a^{\mu m}$ 's span a linear space, as it was assumed in deriving eq 6 and 7, a redundancy condition for  $\Delta r_k$  must also consistently be linear and this rules out terms of the kind given by (8). On the other hand, if displacements  $q_a^{\mu m}$  are considered as true curvilinear coordinates, other terms involving coordinates  $S_p$ , and not only a term of the kind (8), should be included in the force constants (7). Actually this would affect the very definition of internal displacements, as quantities independent of rotation or translation of a repeat unit, but a discussion of this point is beyond the scope of this paper. In what follows we report the results of a normal-mode analysis for ITPP and its deuterio derivatives obtained with force constants derived from eq 6 and 7.

Actual calculations, using a set of translationally symmetrized coordinates of the kind defined in ref 1, were carried out only for a wave vector  $\mathbf{k} = 0$ .

### Normal-Mode Analysis

The crystal structure of ITPP was studied by X-ray diffraction<sup>7</sup> and a reasonable packing of the polymer chains, with the side methyl groups in a *cis* arrangement with respect to the neighboring double bonds, was obtained

Table II  
Observed Spectrum and Values Calculated ( $\text{cm}^{-1}$ ) for Both  
Cis and Skew Forms of an Isolated Chain of Fully  
Deuterated Polypentadiene and Assignment on the Basis  
of Potential Energy Distribution

obsd	calcd		potl energy distrib
	cis form	skew form	
2218	2274	2276	$l(86)$
2219	2219	2219	$l(88)$
2210	2214	2214	$r(92)$
2202	2212	2213	$r(90)$
2180	2183	2183	$d(88)$
2145	2149	2151	$s(86)$
2086	2081	2081	$d(96)$
2070	2076	2076	$r(97)$
1620	1622	1624	$D(69), T(17)$
1200	1210	1193	$T(35), \eta\chi(25), z(25)$
1175	1188	1187	$T(29), \pi(18), \vartheta(16)$
1139	1125	1126	$T(34), \epsilon\varphi\psi(28), \eta\chi(13)$
1100	1091	1109	$\vartheta(24), T(20), \epsilon\varphi\psi(15), z(13)$
1060	1055	1060	$\alpha\beta(78)$
1055	1048	1047	$\alpha\beta(91)$
1045	1046	1046	$\alpha\beta(93)$
1035	1043	1043	$\delta(81)$
1006	996	1005	$\varphi\psi(25), \alpha\beta(17), \eta\chi(14)$
954	962	954	$\varphi\psi(29), \vartheta(21), T(14), \eta\chi(10)$
909	929	915	$\vartheta(28), \eta\chi(19), z(11)$
901	892	899	$\eta\chi(64), T(12), \varphi\psi(12)$
882	843	879	$\vartheta(35), \varphi\psi(21), T(16)$
818	794	779	$\varphi\psi(32), \vartheta(27), \Gamma(23)$
764	760	756	$\alpha\beta(33), \text{rot}(19), \tau_T(11)$
746	723	744	$\Gamma(45), \tau_T(15), \alpha\beta(12), \tau_D(10)$
720	712	709	$\Gamma(49), \tau_D(38)$
692	692	692	$\alpha\beta(40), \eta\chi(33), \tau_T(13)$
647	623	640	$\Gamma(65)$
470	518	473	$\epsilon\varphi\psi(28), \text{rot}(16), \vartheta(11), \Gamma(11)$
422	410	403	$\Gamma(25), \epsilon\varphi\psi(22), \tau_D(13)$
392	358	383	$\pi(45), \epsilon\varphi\psi(12)$
280	274	279	$\text{rot}(47), \tau_T(34)$
	186	180	$\text{rot}(31), \pi(17), \epsilon\varphi\psi(16), \Gamma(15), \tau_T(12)$
	149	151	$\tau_T(85)$
	136	137	$\tau_z(55), \text{rot}(35)$

for orthorhombic space group  $P2_12_12_1$ . These data were used, as discussed in ref 1, to obtain a set of geometrical parameters for the isolated polymer chain in both cis and skew conformations, and normal-mode calculations were carried out accordingly.

Identical calculations have been carried out for ITPP- $d_2$  and ITPP- $d_8$  and are reported in Tables I and II, respectively, where a comparison is made with experimental frequencies taken from the infrared spectra of crystalline samples at room temperature. In these tables an approximate description of each normal mode is reported in terms of quantities obtained from the eigenvectors, calculated for the skew form, and related to elements of the potential energy distribution matrix as described in ref 1. Observed frequencies are better reproduced by values calculated for the skew form, with average errors of 7.8 and  $6.7 \text{ cm}^{-1}$  for the ITPP- $d_2$  and ITPP- $d_8$ , respectively, which are consistently lower than the corresponding values of 15.3 and  $12.0 \text{ cm}^{-1}$  found for the cis form. This result agrees with what was previously found for ITPP and, as in ref 1, is confirmed when we analyze in detail the nature of the normal modes for which large differences occur among frequencies calculated for the two forms. The assignment of C-H and C-D stretching modes is unambiguous for both deuterio derivatives and the same is true for the C=C stretching at 1660 and  $1620 \text{ cm}^{-1}$  for the  $d_2$  and  $d_8$  derivatives, respectively. For ITPP- $d_2$  HCH bending due to the  $\text{CH}_3$  groups is at 1455, 1450, and  $1370 \text{ cm}^{-1}$ , in agreement with the results given in ref 1, while the DCD bending frequency is lowered to  $1041 \text{ cm}^{-1}$ , as easily identified on the basis of the description of the normal modes given in Table I. The corresponding frequencies for the fully deuterated polymer occur between 1060 and  $1035 \text{ cm}^{-1}$ , the lower lying band being clearly due to the  $\text{CD}_2$  group. The =C-H out-of-plane wagging is assigned at  $970 \text{ cm}^{-1}$  for ITPP- $d_2$  as for the undeuterated compound and is shifted at  $720 \text{ cm}^{-1}$  for the fully deuterated derivative.

None of these bands show appreciable differences in the values calculated for the two forms, due to the character of group vibrations, and keep their intensity in the spectrum of the melt. The same is true for other frequencies attributed to group vibrations on the basis of potential energy distribution, although mixing of vibrational coordinates, with coefficients which vary for the three different isotopic species, does not allow a definite assignment as vibrations of particular chemical groups. In Table III we present a list of frequencies in the region 1200–400  $\text{cm}^{-1}$  assigned to fundamental modes which disappear in going from the crystal to the melt. As was done in ref 1, the corresponding bands for deuterated polymers are consid-

Table III  
List of Crystal Frequencies ( $\text{cm}^{-1}$ ) for ITPP, ITPP- $d_2$ , and ITPP- $d_8$ . Absent in the Spectra of the Melted Samples

ITPP		ITPP- $d_2$		ITPP- $d_8$	
obsd	descrip	obsd	descrip	obsd	descrip
1168	$T(33), \alpha\beta(18), \pi(11), \epsilon\varphi\psi(11), \varphi\psi(11)$	1160	$\varphi\psi(25), T(22), \eta\chi(22), \alpha\beta(12)$	1175	$T(29), \pi(18), \vartheta(16)$
1155	$\alpha\beta(28), \epsilon\varphi\psi(14), \varphi\psi(10)$	1126	$\epsilon\varphi\psi(20), \alpha\beta(16), T(14), \eta\chi(10), \vartheta(10)$	1139	$T(34), \epsilon\varphi\psi(28), \eta\chi(13)$
		1110	$T(49), \vartheta(17), \varphi\psi(11), \alpha\beta(10)$	1100	$\vartheta(24), T(20), \epsilon\varphi\psi(15), z(13)$
1109	$z(47), T(12)$	1079	$z(44), \pi(10)$		
1074	$\varphi\psi(37), T(23), \eta\chi(15), \vartheta(15)$			954	$\varphi\psi(29), \vartheta(21), T(14), \eta\chi(10)$
1022	$T(45), \vartheta(15)$	950	$T(26), \vartheta(22), \alpha\beta(21), \eta\chi(11)$	882	$\vartheta(35), \varphi\psi(21), T(16)$
935	$\alpha\beta(45), T(26), \eta\chi(10)$	928	$\alpha\beta(38), T(23), \eta\chi(12)$	692	$\alpha\beta(40), \eta\chi(33), \tau_T(13)$
862	$\Gamma(32), z(29), \tau_T(11), \vartheta(11)$	792	$\Gamma(67), z(16)$	746	$\Gamma(45), \tau_T(11), \alpha\beta(12), \tau_D(10)$
777	$\Gamma(76), \tau_T(13)$	705	$\Gamma(47), \tau_T(21), \vartheta(15)$	647	$\Gamma(65)$
548	$\epsilon\varphi\psi(31), \text{rot}(24), \Gamma(14)$	515	$\epsilon\varphi\psi(31), \text{rot}(23), \vartheta(14)$	470	$\epsilon\varphi\psi(28), \text{rot}(16), \vartheta(11), \Gamma(11)$
476	$\epsilon\varphi\psi(29), \text{rot}(19), \tau_T(13), \eta\chi(12), \Gamma(11)$	452	$\epsilon\varphi\psi(31), \pi(19), \eta\chi(14), \text{rot}(10), \tau_T(10)$	422	$\Gamma(25), \epsilon\varphi\psi(22), \tau_D(13)$
442	$\pi(58), \Gamma(15)$	433	$\pi(50), \Gamma(24), \tau_T(11)$	392	$\pi(45), \epsilon\varphi\psi(12)$

Table IV  
Calculated Frequencies ( $\text{cm}^{-1}$ ) Classified into Irreducible Representations for the Skew Form of ITPP, Including Interchain Potential for Two Different Interaction Ranges

obsd	A		$B_1$		$B_2$		$B_3$	
	6 A	4 A	6 A	4 A	6 A	4 A	6 A	4 A
3025	3034	3034	3034	3034	3034	3034	3034	3034
	3011	3011	3011	3011	3011	3011	3011	3011
	2963	2963	2963	2963	2966	2966	2966	2966
2959	2961	2961	2961	2961	2961	2962	2961	2962
2920	2926	2926	2930	2930	2926	2926	2930	2930
2902	2910	2911	2909	2909	2910	2911	2909	2909
2874	2886	2886	2886	2886	2882	2883	2882	2883
2841	2855	2855	2851	2852	2855	2855	2851	2852
1660	1662	1662	1662	1662	1662	1662	1662	1662
1459	1464	1464	1470	1471	1460	1461	1470	1471
1456	1459	1459	1462	1463	1460	1460	1460	1460
1437	1443	1443	1459	1459	1443	1443	1459	1460
1374	1387	1388	1386	1387	1387	1387	1385	1386
1344	1357	1357	1353	1354	1357	1357	1353	1353
1320	1330	1330	1330	1330	1330	1330	1329	1330
1310	1319	1319	1317	1318	1319	1319	1317	1318
1294	1289	1289	1289	1289	1289	1289	1289	1289
1260	1262	1263	1266	1266	1262	1263	1266	1266
1168	1178	1178	1178	1178	1178	1179	1179	1179
1155	1160	1160	1159	1160	1161	1162	1161	1161
1109	1110	1110	1113	1113	1110	1110	1113	1113
1074	1090	1090	1092	1092	1090	1091	1092	1092
1022	1023	1023	1026	1026	1023	1023	1026	1026
965	985	986	986	986	985	986	986	986
935	945	945	948	949	948	948	950	951
890	921	922	922	923	922	923	924	925
862	869	870	871	871	869	869	870	871
777	768	768	770	770	766	768	770	770
548	575	575	567	568	575	575	567	568
476	462	463	463	463	462	463	463	463
442	440	441	439	439	440	440	438	439
330	347	349	350	351	347	348	349	351
261	229	231	228	229	230	232	229	230
197	198	201	197	201	207	209	206	209
	190	191	190	189	190	191	187	189
	76	82	90	95	68	71	89	94
	63	70	52	54	61	68	34	38
	24	27	11	25	25	30	16	19
	15	20						

ered to be characteristic of the chain regularity and therefore the calculated values may differ in going from one conformation to the other. Appreciable differences are, however, found only for a few bands, as can be seen by inspection of Tables I and II: observed frequencies at 792, 515, and 433 for the  $d_2$  derivative and at 746, 470, and 392  $\text{cm}^{-1}$  for the  $d_8$  derivative are satisfactorily reproduced only by values calculated for the skew form. In particular the calculation favors the skew form in the case of the low frequencies observed at 548 ( $d_0$ ), 515 ( $d_2$ ), and 470 ( $d_8$ )  $\text{cm}^{-1}$  and at 422 ( $d_0$ ), 433 ( $d_2$ ), and 392 ( $d_8$ )  $\text{cm}^{-1}$ . Since the band observed at 548  $\text{cm}^{-1}$  had a low intensity, its assignment to a fundamental mode of ITPP was only tentatively proposed in ref 1. However, as shown in Figure 3, the same absorption pattern is present in the spectra of deuterio derivatives; hence the occurrence of a normal mode with a low intensity at 548  $\text{cm}^{-1}$ , shifted to 515 and 470  $\text{cm}^{-1}$  for  $d_2$  and  $d_8$  derivatives, respectively, is confirmed.

The sequence of calculated values is 561 ( $d_0$ ), 527 ( $d_2$ ), and 473 ( $d_8$ )  $\text{cm}^{-1}$  for the skew form with good overall agreement with the observed values. At 613 ( $d_0$ ), 596 ( $d_2$ ), and 518 ( $d_8$ )  $\text{cm}^{-1}$ , as calculated for the cis form, no band can be observed or, conversely, these predicted values do not match the observed spectra.

Similar behavior is observed for the second band of the doublet shown in Figure 3 at 442 ( $d_0$ ), 433 ( $d_2$ ), and 392 ( $d_8$ )  $\text{cm}^{-1}$  (calculated at 436 ( $d_0$ ), 430 ( $d_2$ ), and 383 ( $d_8$ ) for the skew form and at 402 ( $d_0$ ), 393 ( $d_2$ ), and 358 ( $d_8$ )  $\text{cm}^{-1}$  for the cis form).

Table V  
Calculated Frequencies ( $\text{cm}^{-1}$ ) Classified into Irreducible Representations for the Cis Form of ITPP, Including Interchain Potential for Two Different Interaction Ranges

obsd	A		$B_1$		$B_2$		$B_3$	
	6 A	4 A	6 A	4 A	6 A	4 A	6 A	4 A
3025	3029	3029	3028	3028	3029	3029	3028	3028
	3010	3011	3010	3010	3011	3010	3010	3011
	2965	2965	2965	2965	2968	2968	2968	2968
2959	2961	2962	2961	2962	2963	2963	2963	2963
2920	2952	2952	2953	2953	2952	2952	2953	2953
2902	2913	2913	2911	2912	2913	2913	2911	2912
2874	2888	2888	2888	2888	2883	2883	2883	2883
2841	2855	2855	2855	2855	2855	2855	2855	2855
1660	1658	1658	1658	1658	1658	1658	1658	1658
1459	1466	1466	1466	1466	1461	1462	1461	1462
1456	1459	1460	1459	1460	1461	1461	1461	1461
1437	1439	1439	1441	1442	1439	1439	1441	1442
1374	1389	1390	1390	1390	1388	1389	1388	1389
1344	1359	1360	1361	1361	1359	1360	1361	1361
1320	1353	1353	1353	1353	1353	1353	1353	1353
1310	1282	1282	1281	1281	1282	1283	1281	1282
1294	1278	1279	1279	1279	1278	1278	1279	1279
1260	1263	1263	1262	1262	1263	1263	1262	1262
1168	1193	1193	1194	1194	1194	1194	1195	1195
1155	1159	1159	1159	1160	1160	1160	1160	1160
1109	1098	1099	1096	1097	1099	1099	1097	1097
1074	1080	1080	1078	1079	1080	1081	1079	1080
1022	1027	1028	1027	1028	1028	1028	1028	1028
965	984	985	992	993	984	985	992	993
935	946	946	945	946	950	951	950	950
890	900	901	902	903	901	902	903	904
862	866	866	867	867	864	865	866	866
777	757	758	760	761	757	758	760	761
548	618	618	619	620	619	619	620	620
476	468	469	469	470	469	470	469	470
442	405	406	406	407	404	404	405	406
330	320	321	321	323	320	321	321	323
261	226	228	233	235	229	231	235	237
197	202	205	202	206	211	214	213	216
	174	177	181	183	174	177	181	184
	58	65	67	74	41	46	63	70
	46	56	48	52	27	36	20	23
	18	23	32	39	15	32	15	22
	10	20						

The discussion has so far been given on the basis of the isolated-chain model for the sake of simplicity but, as will be shown in what follows, similar conclusions would be obtained from calculations including interchain forces. Such calculations were carried out by using geometrical parameters, fractional coordinates in units of crystallographic axes, and unit cell parameters as given in ref 7 for the cis form. A reasonable structure for the polymer chain in the skew form was obtained from the proposed cis structure in the following way: first, a rotation of 120° about the  $\text{CH}-\text{CH}(\text{CH}_3)$  single bond was carried out in order to produce a chain in the skew form; next, the same fractional coordinates for the asymmetric carbon atom were assumed as for the crystal of the cis chain, such that the same chain repeat of 4.85 Å was obtained oriented along the  $c$  cell edge; finally the chain was rotated such that the projection of the  $\text{CH}-\text{CH}_3$  bond in the ( $a$ ,  $b$ ) plane was in the same direction as for the cis form. In this way a crystal structure for the skew form was produced, with the same space group as proposed in ref 7, whose crystal energy is calculated at -5.25 kcal/mol, very similar to the value of -4.46 kcal/mol obtained for the cis structure. The interaction potential is of the Buckingham type with semiempirical parameters given by set IV of Williams<sup>8</sup> with interaction centers of H atoms shifted by 0.07 Å toward the C atoms of the C-H bonds. This is the same atom-atom potential used in ref 9 for normal-mode calculations of *trans*-polybutadiene with interchain terms, although, in that case, a first derivative (8) was included

Table VI  
Calculated Frequencies ( $\text{cm}^{-1}$ ) for Both Cis and Skew  
Forms of ITPP- $d_2$ , Including Interchain  
Interactions up to 4 Å

cis form					skew form				
A	B <sub>1</sub>	B <sub>2</sub>	B <sub>3</sub>	obsd	A	B <sub>1</sub>	B <sub>2</sub>	B <sub>3</sub>	
3029	3028	3029	3028		3034	3034	3034	3034	
3011	3010	3011	3010	3012	3011	3011	3011	3011	
2964	2964	2968	2968		2963	2963	2966	2966	
2962	2962	2963	2963	2960	2961	2961	2962	2962	
2929	2929	2929	2929	2920	2911	2911	2911	2911	
2888	2888	2883	2883	2870	2886	2886	2883	2883	
2192	2192	2192	2192	2180	2188	2190	2188	2190	
2091	2091	2091	2091	2090	2089	2086	2089	2086	
1653	1653	1653	1653	1660	1657	1657	1657	1657	
1466	1466	1462	1462	1455	1463	1463	1460	1460	
1460	1460	1461	1461	1450	1459	1459	1460	1460	
1383	1383	1381	1381	1370	1380	1380	1379	1379	
1342	1342	1342	1343	1335	1332	1331	1332	1331	
1319	1319	1319	1319		1317	1315	1317	1315	
1277	1277	1277	1277	1293	1297	1297	1297	1297	
1218	1218	1219	1219	1244	1218	1218	1219	1219	
1169	1170	1170	1171	1160	1167	1166	1168	1167	
1147	1147	1147	1147	1126	1144	1145	1145	1145	
1105	1105	1106	1106	1110	1110	1110	1111	1110	
1061	1062	1062	1062	1079	1091	1093	1091	1093	
1045	1046	1045	1047	1041	1049	1064	1049	1064	
984	991	984	991	970	985	986	985	986	
972	971	973	972	950	967	968	968	969	
943	942	945	944	928	940	942	943	944	
868	868	869	869	883	876	876	876	876	
856	856	856	857	836	837	840	839	840	
774	777	774	777	792	795	797	794	797	
703	704	702	704	705	711	717	711	717	
600	600	600	601	515	540	535	540	535	
437	437	437	437	452	442	442	441	442	
397	398	395	396	433	434	433	434	432	
294	296	295	296	300	322	323	321	322	
225	234	230	236	198	222	220	224	223	
204	205	211	215		200	199	207	206	
174	179	174	179		189	186	190	187	
64	71	46	67		80	92	70	91	
55	51	35	23		69	56	67	38	
23	39	31	22		27	24	30	19	
19					19				

in the expression of force constants. As discussed in the previous section, such a term is not used in the present calculations on ITPP, and a larger interaction range, up to 6 Å for all types of atom-atom contacts, was used to compute the above-mentioned crystal energy.

The computer program used in our calculations needs as an input the fractional coordinates of all atoms in the unit cell, the atomic masses, and the potential energy data, from which a set of force constants is obtained as outlined in the previous section. The space group symmetry is automatically taken into account as the program derives all information about the symmetry from Cartesian coordinates and atomic masses. For each value of  $\mathbf{k}$ , and thus for  $\mathbf{k} = 0$  used in the present calculations, internal and external translationally symmetrized coordinates are projected out of the irreducible representations of the space group of  $\mathbf{k}$  and the secular equation is factorized in block-diagonal form. In Tables IV and V we report calculations of crystal frequencies for both the skew and cis forms of ITPP, classified into irreducible representations of the point group  $D_2$ , isomorphous with the space group of  $\mathbf{k} = 0$ ; these calculations are reported for two different interaction ranges (6 and 4 Å). Since calculated frequencies do not appreciably differ for the two different interaction radii, calculations for ITPP- $d_2$  and ITPP- $d_8$ , as reported in Tables VI and VII, were carried out within the 4-Å interaction range to save computational time.

In agreement with experiment, calculated splittings are

Table VII  
Calculated Frequencies ( $\text{cm}^{-1}$ ) for Both Cis and Skew  
Forms of ITPP- $d_8$ , Including Interchain  
Interactions up to 4 Å

cis form					skew form				
A	B <sub>1</sub>	B <sub>2</sub>	B <sub>3</sub>	obsd	A	B <sub>1</sub>	B <sub>2</sub>	B <sub>3</sub>	
2275	2274	2275	2274		2280	2280	2280	2280	
2220	2220	2221	2221	2218	2220	2220	2220	2220	
2217	2217	2216	2216	2210	2215	2215	2216	2216	
2212	2212	2215	2215	2202	2213	2213	2214	2214	
2197	2198	2197	2198	2180	2187	2189	2187	2189	
2159	2158	2159	2158	2145	2155	2153	2155	2153	
2088	2088	2088	2088	2086	2087	2085	2087	2085	
2081	2081	2077	2077	2070	2079	2079	2077	2077	
1622	1622	1622	1622	1620	1625	1625	1625	1625	
1211	1211	1211	1210	1200	1194	1194	1194	1194	
1188	1188	1188	1188	1175	1188	1188	1188	1188	
1126	1126	1126	1126	1139	1128	1128	1129	1128	
1091	1092	1092	1092	1100	1111	1111	1111	1111	
1057	1057	1056	1056	1060	1061	1066	1061	1065	
1049	1049	1050	1050	1055	1048	1057	1049	1057	
1048	1048	1047	1047	1045	1047	1048	1047	1048	
1044	1045	1044	1046	1035	1046	1047	1046	1047	
1005	1006	1005	1006	1006	1005	1006	1005	1006	
964	964	964	964	954	957	957	957	958	
931	933	931	932	909	920	920	920	920	
898	896	898	896	901	902	902	902	902	
846	846	847	847	882	882	882	882	883	
797	794	797	794	818	781	783	781	783	
762	761	765	764	764	758	761	760	762	
727	728	725	727	746	746	747	747	748	
713	718	713	718	720	712	713	712	713	
694	696	695	696	692	695	697	695	697	
627	628	627	628	647	644	647	644	648	
522	522	523	523	470	486	481	486	481	
411	412	411	412	422	408	408	408	408	
362	363	361	362	392	388	386	387	385	
277	279	277	279	280	294	296	294	295	
191	197	192	197		197	194	197	195	
156	160	158	159		164	162	164	162	
142	144	148	153		143	143	149	149	
61	65	44	63		76	86	67	85	
49	49	32	22		63	52	60	35	
22	37	29	20		26	23	29	18	
18					19				

very small and this supports the validity of a description of the vibrational spectrum in terms of normal modes of the isolated chain.

It is worth noting that appreciable splittings for the infrared-active crystal B modes of internal origin are predicted in the HCH bending region or DCD bending region for deuterated polymers, but only for the skew form. This is in agreement with observation since splittings in this region can be detected in spectra of crystalline samples at liquid nitrogen temperature, as can be verified from Table IV presented in ref 1 and from the corresponding Table VIII of the present paper. In the latter table a list of observed frequencies is given in the region 200–1500  $\text{cm}^{-1}$  for the crystalline samples of ITPP- $d_8$  at two different temperatures and for the corresponding  $d_2$  derivative at room temperature.

Values calculated with included atom-atom interactions are consistently higher by a few wavenumbers than those obtained for the isolated-chain model and this agrees with the experimental result of absorption bands being slightly shifted toward higher frequencies in going from room to low temperature (see Table VIII), where the cell volume decreases and effects of interaction forces are more evident.

The inclusion of interactions among chains obviously produces marked differences in the calculated spectrum for the low-frequency region, if compared with calculations based on a single-chain model. New lattice frequencies are produced due to the introduction of a rotational dis-

Table VIII  
List of Observed Frequencies ( $\text{cm}^{-1}$ ) for Crystalline Samples of ITPP- $d_8$  at Two Different Temperatures and of ITPP- $d_2$  at Room Temperature<sup>a</sup>

polypentadiene- $d_2$ room temp	polypentadiene- $d_8$	
	room temp	liq $\text{N}_2$ temp
198 w	280 w	
300 w	392 m	392 m
433 m	422 m	422 m
452 m	470 vw	471 w
515 vw	647 w	648 m
705 m	692 vw	692 m
792 m	720 vs	725 vs
836 w	746 vs	748 vs
850 vw	764 s	765 vs
883 w	800 vw	804 vw
928 vs	818 m	819 s
950 vs	882 m	883 m
970 vs	901 m	902 s
1041 s	909 s	911 s
1053 vw	935 vw	936 w
1079 m	954 m	957 s
1110 w	1006 vw	1006 w
1126 s	1035 m	1039 m
1160 w	1045 s	1045 s
1244 m		1052 vs
1260 vw	1055 vs	1057 vs
1293 m		1060 vs
1310 vw	1060 vs	1065 vs
1335 m	1078 vw	1080 vw
1370 s	1100 w	1104 m
1450 vs	1139 s	1142 s
1455 vs	1175 w	1180 w
	1200 vw	1203 vw
	1286 vw	1286 vw

<sup>a</sup> vw = very weak, w = weak, m = medium, s = strong, vs = very strong.

placement about the chain axis and of three translations

for each repeat unit.

The crystal field also modifies the description of all other low-lying vibrational modes related to modes with nonzero frequency for the isolated chain and in some case consistently affects the calculated value. In this respect it is interesting to note that a frequency calculated at  $211 \text{ cm}^{-1}$  for the single chain of ITPP is now shifted, by the interchain potential, to  $230 \text{ cm}^{-1}$ . This calculated frequency was not considered characteristic of the chain conformation, as its value is not very sensitive to chain geometry, and was the only one for which a rather large error occurred for both possible chain models. The better fit between calculated and observed values obtained after the inclusion of interchain potential confirms the validity of the calculations and of the internal and external potential adopted in this paper. Although it is not possible to draw conclusions on the crystal structure of ITPP, normal-mode calculations including interchain terms show that the vibrational spectrum cannot be satisfactorily reproduced by using the results of the X-ray analysis,<sup>7</sup> while a good fit occurs for a crystal geometry based on a skew conformation of each polymer chain.

## References and Notes

- (1) N. Neto, M. Muniz-Miranda, E. Benedetti, F. Garruto, and M. Aglietto, *Macromolecules*, preceding paper in this issue.
- (2) N. Neto and C. Di Lauro, *Eur. Polym. J.*, **3**, 645 (1967).
- (3) P. Bardi, Thesis, University of Pisa, 1974.
- (4) L. Lani, Thesis, University of Pisa, 1972.
- (5) M. Kobayashi, *J. Chem. Phys.*, **70**, 4797 (1979).
- (6) N. Neto and D. Kirin, *Chem. Phys.*, **44**, 245 (1979).
- (7) I. W. Bassi, G. Allegra, and R. Scordamaglia, *Macromolecules*, **4**, 575 (1971).
- (8) D. E. Williams, *J. Chem. Phys.*, **47**, 4680 (1967).
- (9) S. L. Hsu, W. H. Moore, and S. Krimm, *J. Appl. Phys.*, **46**, 4185 (1975).

## Notes

### Chiral Discrimination in Poly( $\alpha$ -amino acid)-Metal Complexes

M. DENTINI and P. De SANTIS\*

*Istituto di Chimica Fisica, Università di Roma, Roma, Italy*

M. SAVINO

*Centro di Studio per gli Acidi Nucleici del CNR Istituto di Fisiologia Generale, Università di Roma, Roma, Italy.*

Received April 18, 1979

The conformational order and rigidity that generally characterize the state of poly( $\alpha$ -amino acids) in solution and their intrinsic chirality provide a unique opportunity for investigating topochemical effects such as stereospecificity and stereoselectivity in reactions occurring on such protein-like matrices. In fact, polypeptide systems having functional side chains are capable of stereospecifically binding square-planar prochiral metal complexes at pairs of amino acid residues along the chain.<sup>1-3</sup>

We report our CD and ESR investigations of the influence of chiral and conformationally rigid polypeptide matrices on the structure of anchored metal complexes. The right-hand side of Figure 1 illustrates the polypeptide matrices used. These are bound via Schiff bases of salicylaldehyde or pyridoxal with ornithine and lysine side

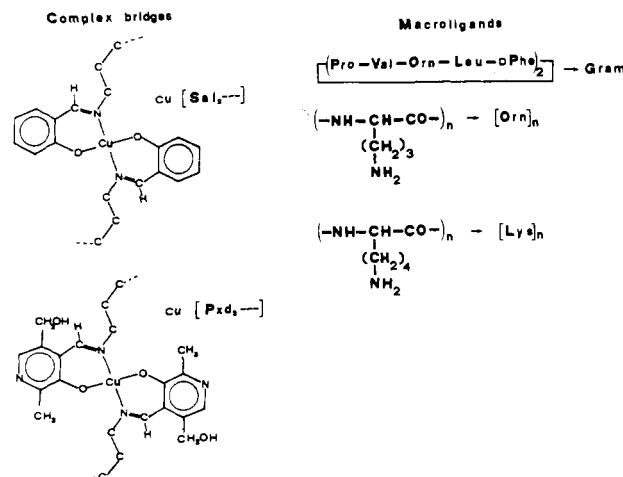


Figure 1. Macroligands (right) and complex bridges (left) investigated.

chains; the complex bridges are indicated on the left-hand side.

Under the experimental conditions adopted (room temperature; methanol, trifluoroethanol [apparent pH 7], chloroform, *N,N*-dimethylformamide [DMF], and trimethyl phosphate [TMP] organic solvents) the confor-